Heat and Mass Transfer Research Journal
Vol. 2, No. 2; 2018
Published by CanSRG
http://cansrg.com/journals/hmtrj/

Power-Law Heat Transfer on Linearly Stretching or Shrinking Surfaces

Patrick Weidman

Department of Mechanical Engineering, University of Colorado, Boulder, CO 80309-0427

Abstract

The heat transfer from a linearly stretching surface with power-law temperature variation along the surface is considered for both stretching and shrinking surfaces. For stretching sheets this extends previous works to large temperature exponents and reveals new exact solutions. Here for the first time shrinking sheets are considered for the dual solutions that exist in the presence of suction. It is proven that only the upper branch of the dual solutions is stable. Thus only the upper branch is viable and results are given at various points along this branch which exhibit discontinuities with increasing values of the temperature exponent. These discontinuities separate heat transfer away from the wall to heat transfer to the wall.

Keywords: *stretching/shrinking surface; power-law temperature; shear stress; heat transfer.*

1. Introduction

Many researchers have studied problems related to flow over stretching, and sometimes shrinking sheets. Some include the effects of heat transfer, suction and blowing and stagnation-point flow. For example, a general study of stagnation-point flows impinging on linearly and radially stretching surfaces was reported by Weidman and Turner [1] and Weidman [2] considered the problem of Hiemenz stagnation-point flow impinging on a biaxially stretching surface.

In the present study we are interested in the heat transfer from stretching surfaces in the absence of an outer streaming flow. Although problems have been investigated for convective flow along vertical stretching surfaces — see Patil, et al [3] and Gorla and Sidawi [4] — we restrict our discussion to horizontal surfaces. In particular, we consider linearly stretching and linearly shrinking surfaces with associated wall temperature varying as a power-law of the distance along the plate. Crane [5] was the first to provide a solution for a linearly stretching plane with a uniformly heated surface. The problem of power-law temperature variation along a linearly stretching plate was first considered by Grubka and Bobba [6]. Subsequently, Chen and Char [7,8] and Ali [9,10] have extended this problem to include the effects of power-law stretching surfaces, non-Newtonian flow, and transpiration through the porous surface. For temperatures varying with downstream distance as x^n, the above studies have been limited to exponents in the range $-3 \le n \le 3$.

The goal of the present investigation is to extend results to $n = 20$ for stretching sheets and to consider, for the first time, power-law temperature variations along a shrinking sheet. Miklavcic and Wang [6] were the first to consider the flow induced by a shrinking sheet and found that suction was necessary to maintain the flow. Denoting f_0 as the suction parameter they found dual solutions for all $f_0 > 2$, a unique solution for $f_0 = 2$ and no solutions for $f_0 < 2$. In this paper we prove that only the upper branch of the dual solutions is stable. Solutions are reported along the

Submitted: January 30, 2018 Revised: July 11, 2018 Accepted: July 12, 2018

upper viable branch at selected values of the suction parameter for various values of the temperature exponent. We find that the flow alternates between heat transfer from the wall to heat transfer to the wall as the exponent *n* increases.

The presentation is as follows. In §2 the problem is formulated. The problem for stretching plates is analyzed in §3 and that for shrinking plates is given in §4. The stability of the dual solutions encountered for a shrinking surface is presented in an Appendix and a discussion with concluding remarks are given in §5.

2. Problem Formulation

We consider a modification and generalization of the problem of a linearly stretching plate studied by Crane [5]. Crane considered heat transfer from a plate with uniform wall temperature. Here we posit temperature with power-law variations in the direction of flow and also include the case of a linearly shrinking plate.

We take Cartesian coordinates (x, y) with corresponding velocities (u, v) and temperature T. At the wall, we presume linear stretching and power-law temperature variations of the form

$$u(x,0) = ax, \qquad v(x,0) = 0, \qquad T(x,0) = bx^n + T_\infty \tag{1}$$

where $a > 0$ corresponds to a stretching plate, $a < 0$ corresponds to a shrinking plate, and T_∞ is the uniform temperature in the far field. The continuity equation, the two-dimensional boundary-layer equations for zero pressure gradient in the quiescent far field, and the heat equation are given as

$$u_x + v_y = 0 \tag{2a}$$

$$uu_x + vu_y = vu_{yy} \tag{2b}$$

$$uT_x + vT_y = \kappa T_y y \tag{2c}$$

where ν is the kinematic viscosity, $\kappa = k/\rho c_p$ is the thermal diffusivity in which k is the thermal conductivity and c_p the specific heat at constant pressure.

We now posit the solution form satisfying the continuity equation as

$$u(x,y) = ax\acute{f}(\eta), \qquad u(x,y) = -\sqrt{av}\, f(\eta), \qquad T(x,y) = bx^n\theta(\eta) + T_\infty, \quad \eta = \sqrt{a/\nu y} \tag{3}$$

Inserting this into the governing equations (2) gives the one way coupled ordinary differential equations

$$f''' + f\, f''' - f'^2 = 0 \tag{4a}$$

$$\theta'' + Pr(f\theta' - nf'\theta = 0 \tag{4b}$$

in which $Pr = \nu/\kappa$ is the Prandtl number. We consider stretching and shrinking plates separately in the following sections.

Of interest is the wall shear stress is given by

$$T = \mu \frac{\partial u}{\partial y}\Big|_{y=0} = \rho \nu^{1/2} a^{3/2} x f''(0) \tag{5}$$

and also, the wall heat transfer is

$$q = k \frac{\partial T}{\partial y}\Big| y = 0 = -kb\sqrt{\frac{a}{\nu}}\, x^n \theta'(0) \tag{6}$$

3. Linearly stretching plates

For linearly stretched plates, Eqs. (4) are to be solved with boundary and far field conditions

$$f(0) = 0, \qquad f'(0) = 1, \qquad f'(\infty) = 0, \qquad \theta(0) = 1, \qquad \theta(\infty) = 0 \tag{7}$$

The solution of the Crane stretching problem (4a) is $f(\eta) = 1 - e^{-\eta}$ and insertion into the heat equation (4b) gives

$$\theta'' + Pr[(1 - e^{-\eta})\theta' - ne^{-\eta}\theta] = 0 \tag{8}$$

Although a first integral exists, one must ultimately resort to numerical calculation for solutions when $Pr \neq 1$. Note that solutions here depend on two parameters, namely the Prandtl number Pr and the temperature exponent n. However, in the case $Pr = 1$ for which the boundary-value problem is

$$\theta'' + (1 - e^{-\eta})\theta' - ne^{-\eta}\theta = 0, \qquad \theta(0) = 1, \qquad \theta(\infty) = 0 \tag{9}$$

an exact solution exists given by

$$\theta(\eta) = e^{-\eta}\frac{U(1-n,2,-e^{-\eta})}{U(1-n,2,-1)} \tag{10}$$

where $U(a, b, z)$ is the Kummer confluent hypergeometric function; see Abramowitz and Stegun [12]. Note that n need not be an integer.

Two simple forms of (10) exist. First, for $n = 0$ corresponding to uniform wall temperature, Crane [5] found

$$\theta(\eta) = \frac{e}{e-1}\left(1 - e^{-e^{-\eta}}\right) \tag{11}$$

and for $n = 1$ the solution is simply

$$\theta(\eta) = e^{-n} \tag{12}$$

Another exact solution was uncovered during the numerical integrations to be presented in the next section. While integrating for $Pr = n = 10$ one finds $\theta'(0) = -10$. Also, solution (12) shows that at $Pr = n = 1$ the wall temperature gradient $\theta'(0) = -1$ is found. This led to a new exact solution for all $Pr = n$ of the form

$$\theta(\eta) = e^{-n\eta} \tag{13}$$

Sample exact solutions $\theta(\eta)$ at $Pr = 1$ are provided in figure 1.

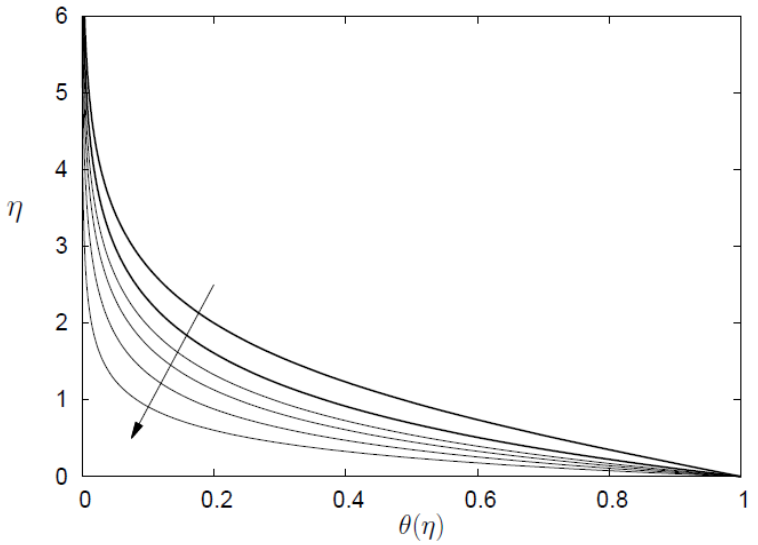

Figure 1. Similarity temperature profiles $\theta(\eta)$ for stretching at $Pr = 1$ for exponent values $n = \{0, 1, 2, 3, 5, 10\}$. The arrow points in the direction of increasing n and the bold line profiles are the exact solutions given by Eqs. (11) and (12).

3.1. Numerical results

Numerical calculations were performed using the integrator package ODEINT in Press, et al. [13]. Integration lengths were varied to ensure solution independence of integration length.

A study of the stretching wall problem was carried out for the three Prandtl number $Pr = \{1, 5, 10\}$ varying the temperature exponent n. Results for the wall heat transfer parameter $\theta'(0)$ are given in figure 2. The closed symbols in this figure pertain to results obtained from the exact solution for $Pr = n$ given in Eq. (13). Note the limit to zero wall heat transfer at $n = -1$. This motivates looking for an exact solution at $n = -1$ which is found to be

$$\theta(\eta) = e^{Pr}\left[e^{-Pr(\eta+e^{-\eta})}\right] \tag{14}$$

which furnishes the wall heat transfer result $\theta'(0) = 0$.

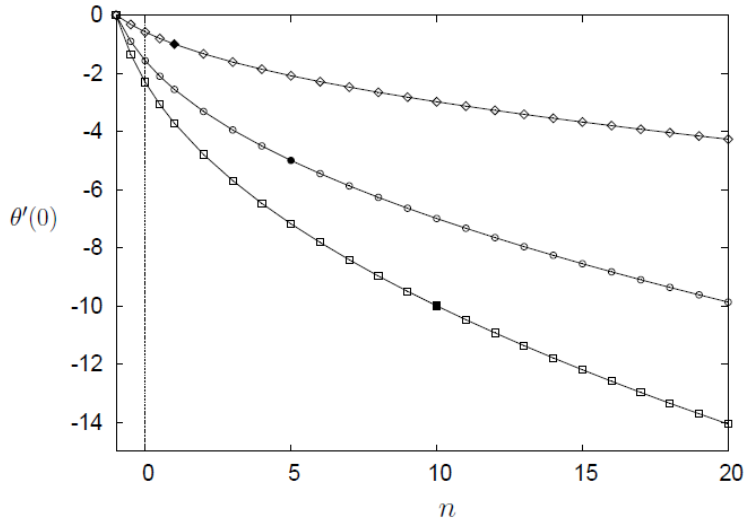

Figure 2. Stretching plate results showing the wall temperature gradient $\theta'(0)$ plotted as a function of the temperature exponent n for $Pr = \{1, 5, 10\}$ with diamonds for $Pr = 1$, circles for $Pr = 5$ and squares for $Pr = 10$. The solid points denote exact results derived from Eq. (13).

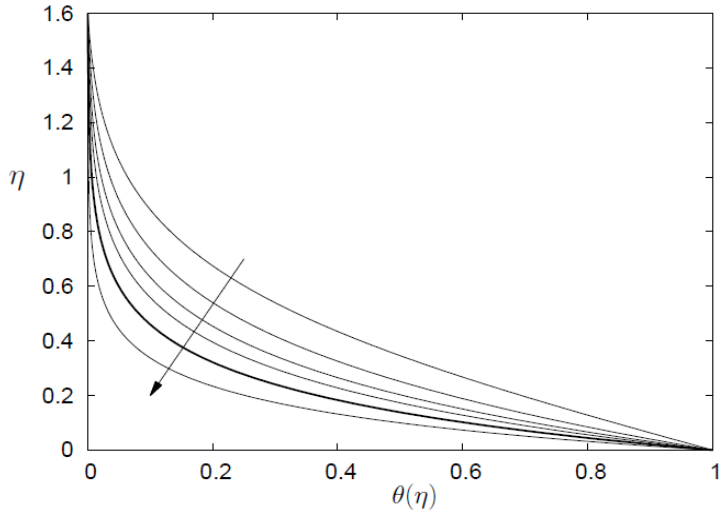

Figure 3a. Similarity temperature profiles $\theta(\eta)$ for stretching at $Pr = 5$ for exponent values $n = \{0, 1, 2, 3, 5, 10\}$. The arrow points in the direction of increasing n and the bold line profile is the exact solution given by Eq. (13) for $n = 5$.

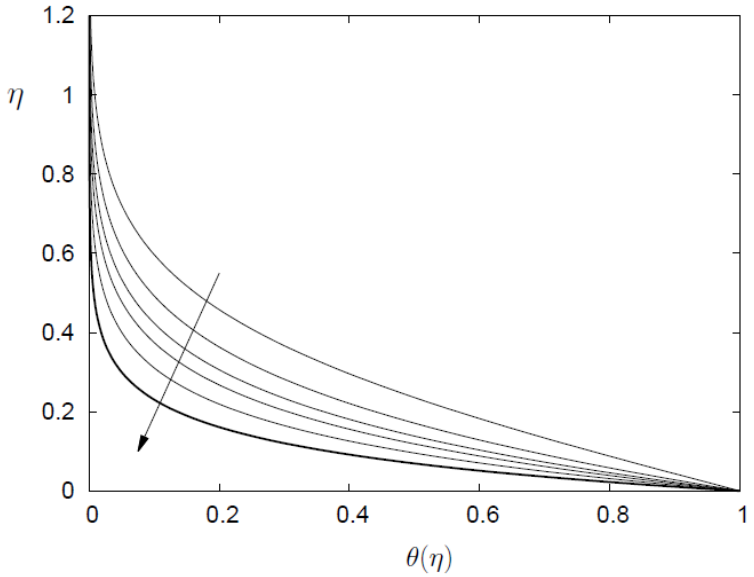

Figure 3b. Similarity temperature profiles $\theta(\eta)$ for stretching at Pr = 10 for exponent values n = {0, 1, 2, 3, 5, 10}. The arrow points in the direction of increasing n and the bold line profile is the exact solution given by Eq. (13) for n = 10.

Sample velocity profiles for $Pr = 5$ are displayed in figure 3a and profiles for $Pr = 10$ are shown in figure 3b. Comparison of results in figures 1 and 3 shows that the temperature boundary layer thickness decreases with increasing Prandtl number.

4. Linearly shrinking plates

Solutions for shrinking plates require suction to maintain the flow. In this case the appropriate boundary and far-field conditions for Eq. (4a) are

$$f(0) = f_0, \qquad f'(0) = -1, \qquad f'(\infty) = 0, \qquad \theta(0) = 1, \qquad \theta(\infty) = 0 \qquad (15)$$

where $f_0 > 0$ corresponds to suction which is the required form of solution.

The solution of (4a) is then found to be (Miklavcic and Wang [11])

$$f(\eta) = f_0 + \frac{e^{-\alpha\eta}-1}{\alpha} \qquad (16)$$

where

$$f''(0) = \alpha_{\pm} = \frac{f_0 \pm \sqrt{f_0^2-4}}{2} \qquad (17)$$

and the subscripts $\{\pm\}$ denote upper and lower branch solutions. A plot of the wall shear stress $f''(0)$ as a function of the suction parameter f_0 on both branches is given in figure 4. The stability analysis presented in the Appendix shows that the upper branch is stable whilst the lower branch is unstable. Thus, henceforth we will only consider $\alpha_+ \equiv \alpha = f''(0)$ corresponding to the stable upper branch solution. In this case we insert solution (16) into the heat equation (4b) to obtain

$$\theta'' + Pr\left[\left(f_0 + \frac{e^{-\alpha\eta}-1}{\alpha}\right)\theta' + ne^{-\alpha\eta}\theta\right] = 0 \qquad (18)$$

to be solved with boundary and far-field conditions on $\theta(\eta)$ as given in (15). Notice that now for shrinking plates there are three parameters involved, namely the Prandtl number Pr, the temperature exponent n and the suction parameter f_0 which is known over the region of existence of solutions varying from.

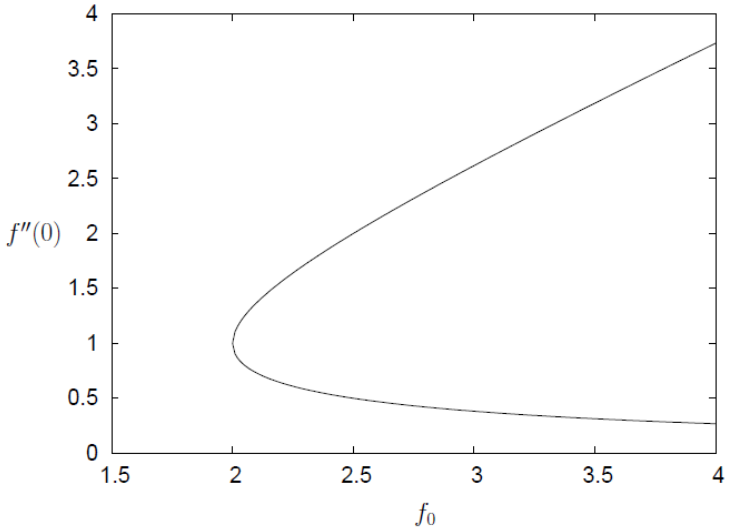

Figure 4. Dual solution branches for the shrinking plate plotting the wall shear stress parameter $f''(0)$ against the suction parameter f_0. The analysis in the Appendix shows that only the upper solution branch is stable.

While solutions exist for all $f_0 \geq 2$, the only exact solution found is for $Pr = 1$ at the turning point at $f_0 = 2$. In this case the solution for any n is given by

$$\theta(\eta) = e^{-\eta}\,\frac{U(1-n,2,e^{-\eta})}{U(1-n,2,1)} \tag{19}$$

where again $U(a, b, z)$ is the Kummer confluent hypergeometric function. A simpler solution exists for $n = 1$ which is given by

$$\theta(\eta) = \frac{e^{e-\eta}-1}{e-1} \tag{20}$$

A plot of dimensionless temperature profiles $\theta(\eta)$ at the value $f_0 = 2$ is provided in figure 5 for selected values of n. Note the change of sign in $\theta'(0)$ that occurs across $n = 2$.

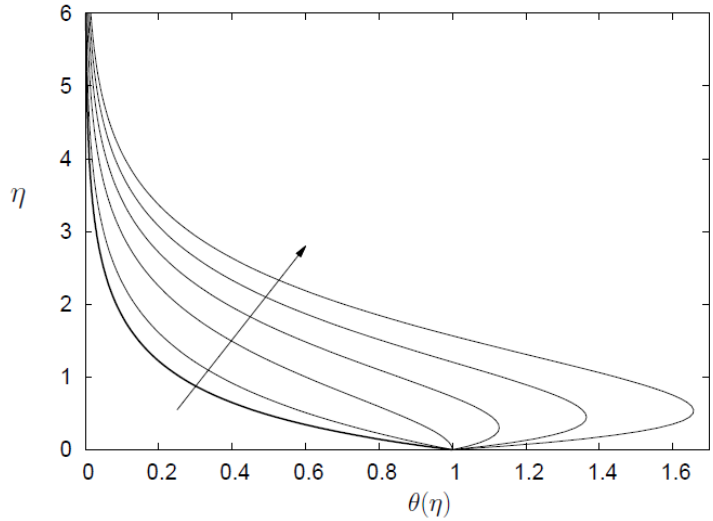

Figure 5. Similarity temperature profiles $\theta(\eta)$ for shrinking at $Pr = 1$ and $f_0 = 2.0$ for exponent values $n = \{0, 1, 2, 2.5, 2.8, 3\}$. The arrow points in the direction of increasing n and the bold line profile is the exact solution given by Eq. (20)

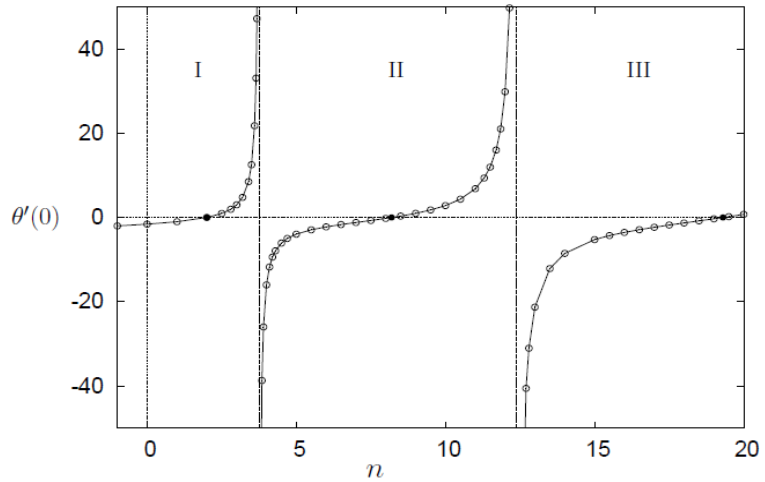

Figure 6a. Wall temperature gradient $\theta'(0)$ at f_0 = 2.0 plotted as a function of the temperature exponent n for Pr = 1 in which the solid points indicate zero wall heat transfer.

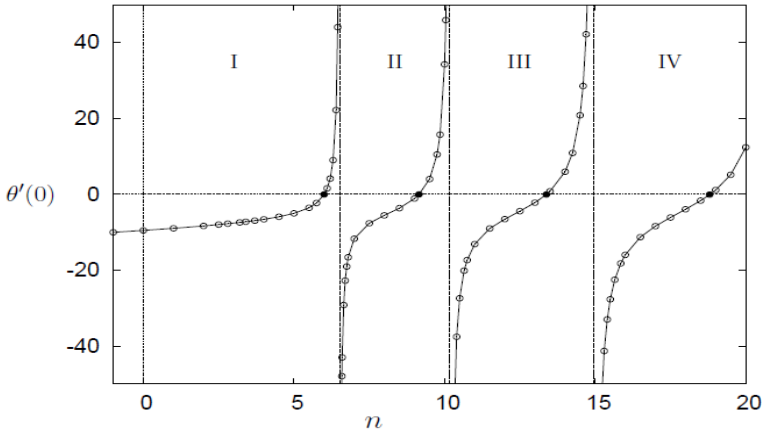

Figure 6b. Wall temperature gradient $\theta'(0)$ at f_0 = 2.0 plotted as a function of the temperature exponent n for Pr = 5 in which the solid points indicate zero wall heat transfer.

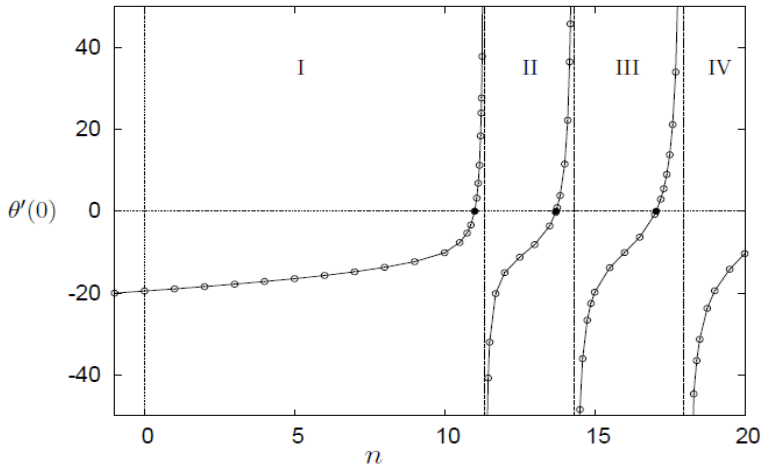

Figure 6c. Wall temperature gradient $\theta'(0)$ at f_0 = 2.0 plotted as a function of the temperature exponent n for Pr = 10 in which the solid point indicates zero wall heat transfer.

4.1. Numerical results

Here we have three parameters, so we will compute $\theta'(0)$ versus the temperature exponent n for the same three Prandtl numbers $Pr = \{1, 5, 10\}$ as for the stretching plate problem, only now do it for selected values of the suction parameter f_0. The four selected values of f_0 considered and the corresponding values of $f''(0)$ on the upper stable branch are listed in Table 1.

Table 1. The four selected values of f_0 considered for shrinking plates and the corresponding values of $f''(0)$.

f_0	$f''(0)$
2.0	1.000
2.5	2.000
3.0	2.618
4.0	3.732

We start with the turning point value $f_0 = 2.0$ for which $f''(0) = 1.0$. According to the stability analysis in the Appendix, this is a point of neutral stability. These results for the wall temperature gradient $\theta'(0)$ are given in three plots: figure 6a for $Pr = 1.0$, figure 6b for $Pr = 5.0$ and figure 6c for $Pr = 10.0$. The interesting feature here is the appearance of singularities across which the wall temperature gradient changes sign, and between which there are also zero crossings in $\theta'(0)$ A plot of these features is presented in figure 7. Sample temperature profiles in regions I, II, II and IV shown in figures 8a,b,c respectively corresponding to $Pr = \{1, 5, 10\}$. The solid lines show profiles for heat transfer from the wall to the fluid and the dashed liens show profiles for heat transfer from the fluid to the wall.

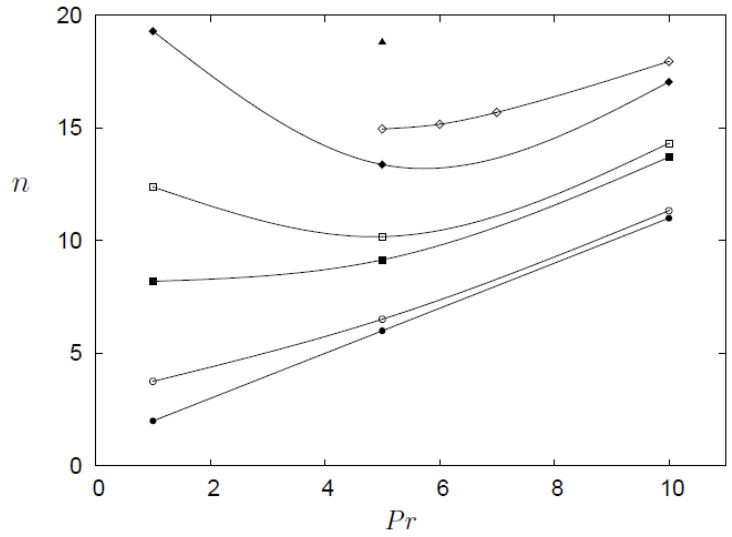

Figure 7. Cross plot for $f_0 = 2.0$ of temperature exponents n at the zero and singular points found in figures 6a, b, c. The solid circles, squares, diamonds and triangles show the Prandtl number variation of the first, second, third and fourth zeros of $\theta'(0)$. The open circles, squares and diamonds show the Prandtl number variation of the singular values of $\theta'(0)$.

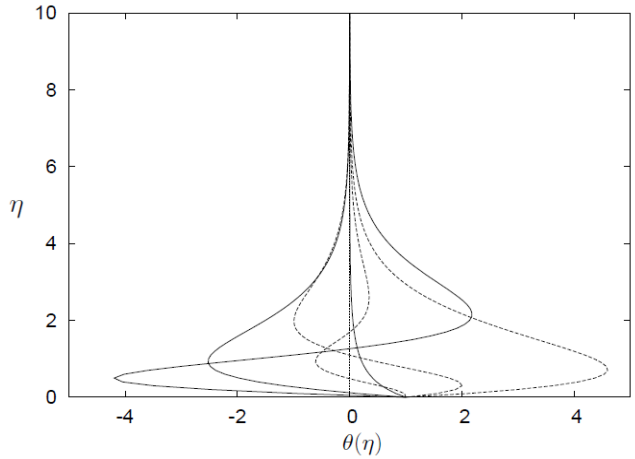

Figure 8a. Similarity temperature profiles $\theta(\eta)$ at f_0 = 2.0 for the shrinking plate at Pr = 1. The sold lines for n = {3.5, 11, 20} correspond to heat transfer from the wall to the fluid while the dashed lines for n = {−1.0, 4.2, 13} correspond to heat transfer from the fluid to the wall.

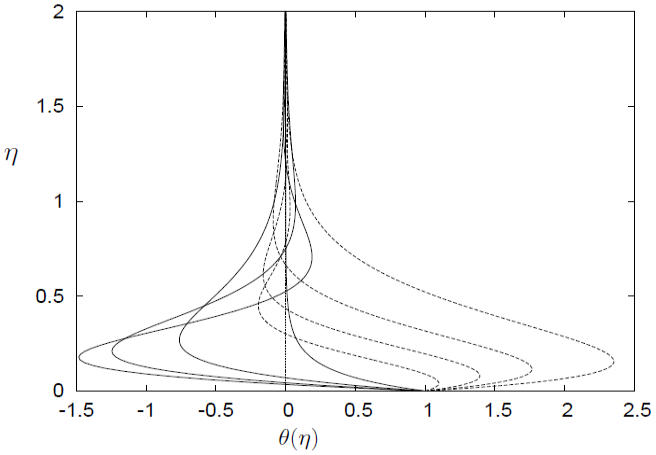

Figure 8b. Similarity temperature profiles $\theta(\eta)$ at f_0 = 2.0 for the shrinking plate at Pr = 5. The sold lines for n = {6.4, 9.85, 14.25, 19.5} correspond to heat transfer from the wall to the fluid while the dashed lines for n = {−1.0, 6.75, 10.5, 15.4} correspond to heat transfer from the fluid to the wall.

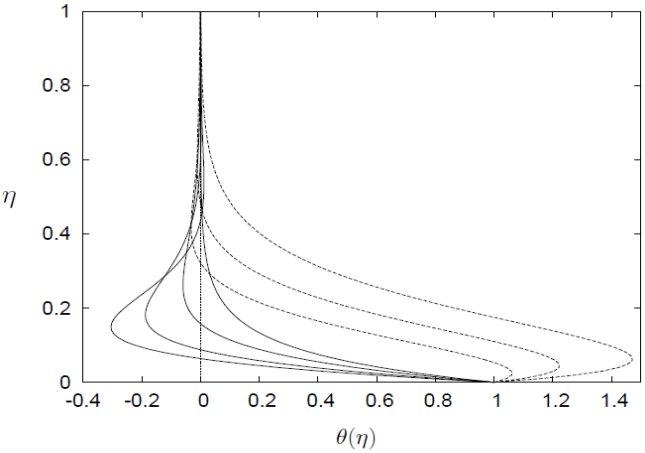

Figure 8c. Similarity temperature profiles $\theta(\eta)$ at f_0 = 2.0 for the shrinking plate at Pr = 10. The sold lines for n = {11.2, 14, 17.3} correspond to heat transfer from the wall to the fluid while the dashed lines for n = {9, 12, 15, 18.75} correspond to heat transfer from the fluid to the wall.

We now move on to higher values of f_0. Figure 9 shows results for $f_0 = 2.5$, figure 10 shows results for $f_0 = 3.0$ and figure 11 shows results for $f_0 = 4.0$. Clearly, over the range $-1 \le n \le 20$ there are tow singularities for $f_0 = 2.5$, but these disappear for the strong suction values $f_0 = 3$ and $f_0 = 4$. Sample temperature profiles for $f_0 = 4$ at $Pr = \{1, 5, 10\}$ are given in figure 12.

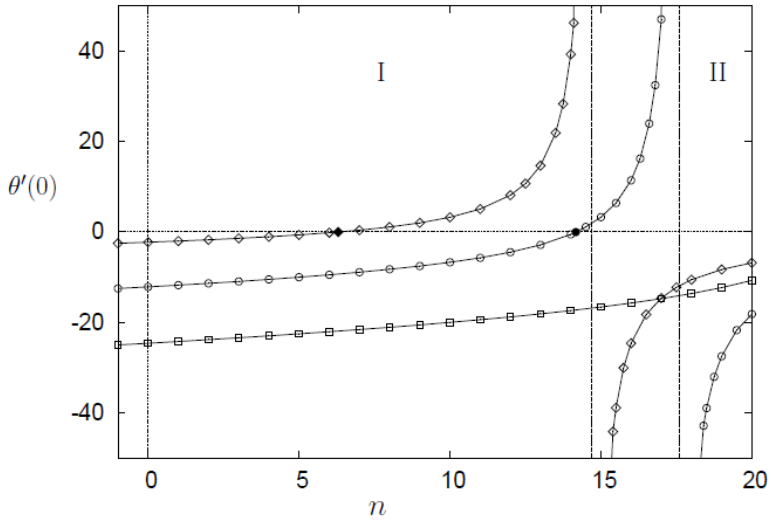

Figure 9. The $f_0 = 2.5$ wall temperature gradient $\theta'(0)$ plotted as a function of the temperature exponent n for $Pr = \{1, 5, 10\}$ with diamonds for $Pr = 1$, circles for $Pr = 5$ and squares for $Pr = 10$. The solid points indicate zero wall heat transfer.

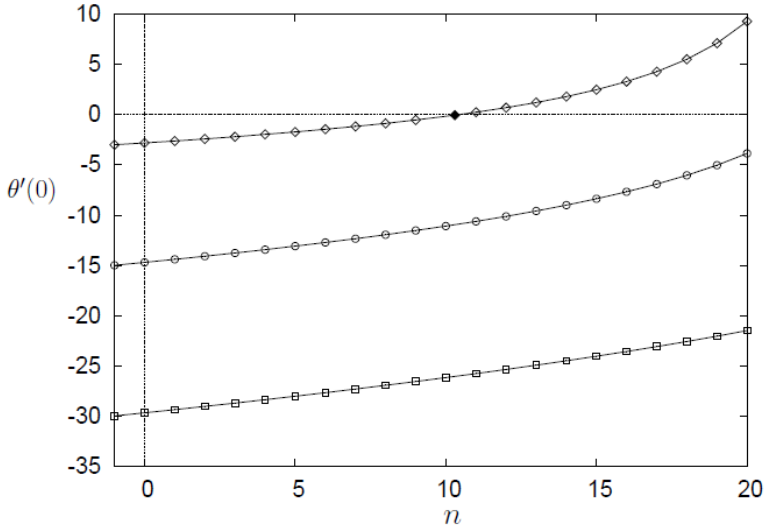

Figure 10. The $f_0 = 3.0$ wall temperature gradient $\theta'(0)$ plotted as a function of the temperature exponent n for $Pr = \{1, 5, 10\}$ with diamonds for $Pr = 1$, circles for $Pr = 5$ and squares for $Pr = 10$. The solid point indicates zero wall heat transfer.

5. Discussion and Conclusion

We have considered the flow and heat transfer induced by a stretching or shrinking sheet under the influence of wall temperatures that increase as bx^n. For stretching sheets studied by Grubka and Bobba [6], Chen and Char [7,8], Ali [9,10] we have extended their work by increasing the

exponent to $n = 20$ and have reported new exact solutions. In particular there is a simple exact solution for the case $Pr = n$ given by Eq. (13).

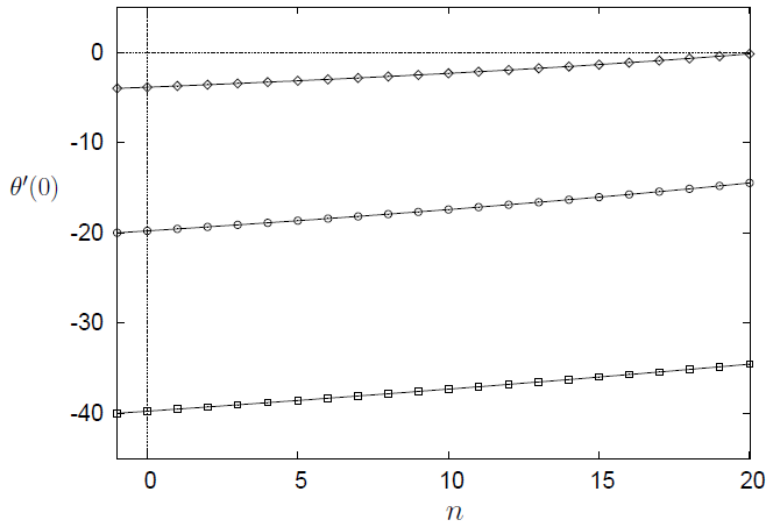

Figure 11. The $f_0 = 4.0$ wall temperature gradient $\theta'(0)$ plotted as a function of the temperature exponent n for $Pr = \{1, 5, 10\}$ with diamonds for $Pr = 1$, circles for $Pr = 5$ and squares for $Pr = 10$.

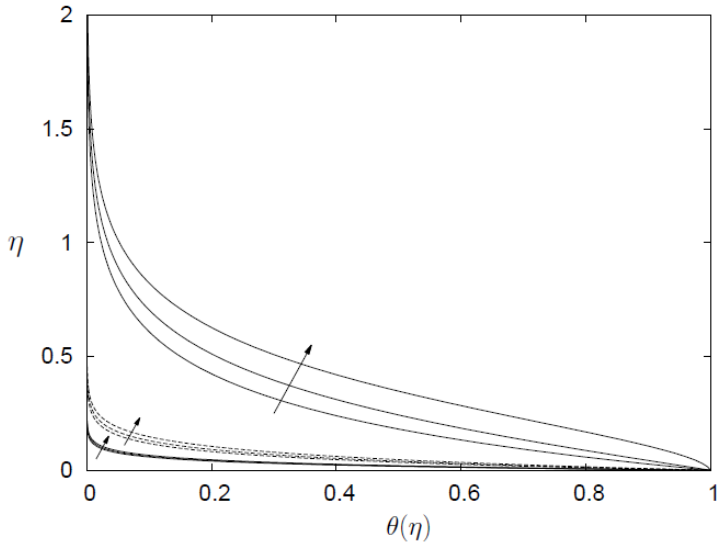

Figure 12. Similarity temperature profiles $\theta(\eta)$ at $f_0 = 4.0$ for the shrinking plate at $Pr = \{1, 5, 10\}$ plotted for $n = \{0, 10, 20\}$. The upper bold lines for $Pr = 1$, the middle-dashed lines are for $Pr = 5$ and the lower thin lines are for $Pr = 10$ with arrows in the directions of increasing values of n.

For an isothermal shrinking surface, Miklavcic and Wang [11] showed that suction must be present and found dual solutions for all $f_0 \geq 2$. In the Appendix we have analyzed the stability of these solutions and find that only the upper branch is stable. Thus, for the first time, we perform a study of solutions for a shrinking sheet along the upper branch at selected values of f_0 with power-law temperature variations up to $n = 20$. The value $f_0 = 2$ is neutrally stable and reveals complicated temperature variations with increasing n. For this critical value, discontinuities in the wall temperature gradient exists separating regions of heat transfer to and from the wall. Also, there are

zero crossings between the singularities that also separate regimes of heat transfer to and from the wall. The regions between discontinuities labeled I, II, III and IV behave as tangent functions but with periods increasing with n; see figure 6a,b,c. As the transpiration parameter is increased to $f_0 = 2.5$ only the regions I and II appear, and for $f_0 = 3$ and 4 the discontinuities disappear completely, at least in the region $-1 \le n \le 20$ studied here.

Sample temperature profiles for stretching sheets at $Pr = 1$ shown in figure 1 exhibit monotone behavior and similar profiles exist for $Pr = 5$, 10. For shrinking sheets, on the other hand, the temperature profiles shown in figures 8a,b,c for $f_0 = 2.0$ display signatures of heat transfer from the wall to the fluid (solid lines) and from the fluid to the wall (dashed lines). This feature is still apparent for $f_0 = 2.5$ but disappears for $f_0 = 3$ and 4 in the range $-1 \le n \le 20$ studied here. The curious feature of the existence of discontinuities in the wall temperature gradient for shrinking surfaces is linked to the neutral stability feature of $f_0 = 2.0$ but this feature abates as f_0 increases. We have not been able to provide a physical explanation for the appearance of the discontinuities with increasing values of n which separate regimes of heat transfer to and from the wall. Perhaps an explanation of this feature can be obtained in the future, but heat transfer from the outer ambient to the wall seems to be not physically realizable.

6. Appendix

We now ascertain the stability for linear shrinking plates where dual solutions exist. Thus, we need to include the temporal acceleration in the momentum equation which is done by positing the solution as

$$u(x,\eta,\tau) = a\, x\, f'(\eta,\tau) \tag{A.1}$$

where $\tau = a\, t$ and the prime still denotes differentiation with respect to η. Inserting this into the unsteady momentum equation gives

$$f''' + f\, f'' - f'^2 - f'_\tau = 0 \tag{A.2}$$

Following Merkin [14] we study the temporal stability of solutions by inserting

$$f(\eta,\tau) = f_1(\eta) + g(\eta) e^{-\lambda\tau} \tag{A.3}$$

into (A.2) assuming $|g(\eta)| \ll |f_1(\eta)|$ for small disturbances. The leading order term gives the original equation for $f(\eta)$, and the first-order correction gives rise to the boundary value problem

$$g''' + f_1\, g'' - 2 f_1' g' + f_1'' g + \lambda g' = 0 \tag{A.4a}$$

$$g(0) = 0, \qquad g'(0) = 0, \qquad g'(\infty) = 0 \tag{A.4a}$$

Solutions are obtained setting $g''(0) = 1$ and varying λ to satisfy the far field condition in (A.4b). Solution of (A.4) give an infinite set of eigenvalues $\lambda_1 < \lambda_2 < \lambda_3 < \dots$; if the smallest eigenvalue λ_1 is negative, there is an initial growth of disturbances and the flow is unstable; when λ_1 is positive, there is an initial decay and the flow is stable.

In our problem $f_0 = 2$ is a turning point in the solutions and corresponds to a point of neutral stability. For values of f_0'' exhibiting a turning point, local theory of the saddle-node bifurcation is sufficient to ensure that, generically, there is a transition of stability across each turning point; see, for example, Kuznetsov [15]. Thus, stability of one branch of solutions infers instability of the other branch. The lowest eigenvalues at selected points on the upper branch have been calculated with sample results as shown in Table 2. Since the results show that $\lambda_1 > 0$, the upper branch solution is stable whilst the lower branch is unstable.

Table 2. Lowest eigenvalue λ_1 at selected values of f_0 on the upper branch solution.

f_0	λ_1
2.50	1.0374
3.00	1.7677
3.50	2.5182
4.00	3.2316

References

[1] P. D. Weidman and M. Turner, Stagnation-point flow with stretching surfaces: A unified formulation and new results, Euro. J. Mech. B/Fluids, vol 61, pp. 144-153, 2017.

[2] P. D. Weidman, Hiemenz stagnation-point flow impinging on a biaxially stretching surface, Meccanica, DOI 10.1007/s11012-017-0761-7, 2017.

[3] P. M. Patil, S. Roy and A. J. Chamkha, Mixed convection flow over a vertical power-law stretching surface, Int. J. Num. Methods Heat Fluid Flow, vol 20, pp. 445-458, 2010.

[4] R. S. R. Gorla and I. Sidawi, Free convection on a vertical stretching surface with suction and blowing, Flow, Turbulence and Combustion, vol 52, pp. 247-257, 1994.

[5] L. J. Crane, Flow past a stretching plate, Kurz Mitteilungen, vol 21, pp. 645-647, 1970.

[6] L. J. Grubka and K. M. Bobba, Heat transfer characteristics of a continuous stretching surface with variable temperature, ASME Transactions, vol 107, pp. 248-250, 1985.

[7] C.-K. Chen and M.-I. Char, Heat transfer of a continuous, stretching surface with suction and blowing, J. Math. Anal. Appl., vol 135, pp. 568-580, 1988.

[8] C.-K. Chen and M.-I Char, Temperature field in non-Newtonian flow over a stretching plate, J. Math. Anal. and Appl., vol 151, pp. 301-307, 1990.

[9] M. Ali, Heat transfer characteristics of a continuous stretching surface, Warme- und Stoffubertragung, vol 29, pp. 227-234, 1994.

[10] M. Ali, On thermal boundary layer on a power-law stretched surface with suction or injection, Int. J. Heat and Fluid Flow, vol 16, pp. 280-290, 1995.

[11] M. Miklavcic and C. Y. Wang, Viscous flow due to a shrinking sheet, Quart. Appl. Math., vol 64, pp. 283-290, 2006.

[12] M. Abramowitz and I. Stegun, Handbook of Mathematical Functions, U. S. Government Printing Office, Washington, DC, 1972.

[13] W. H. Press, B. P. Flannery, W. A. Teukolsky and W. T. Vetterling, Numerical Recipes, Cambridge University Press, Cambridge, 1989.

[14] J. H. Merkin, On dual solutions occurring in mixed convection in a porous medium, J. Engrg. Math., vol 2, 171-179, 1985.

[15] Y. A. Kuznetsov, Elements of Applied Bifurcation Theory, third ed., Springer, New York, 2004.